ARTICLES

Transient Hole Burning in the Infrared in an Ethanol Solution

R. Laenen,* C. Rauscher, and A. Laubereau

Physik-Department E11, Technische Universität München, D-85748 Garching, Germany

Received: June 12, 1996; In Final Form: January 21, 1997[⊗]

Transient hole burning in the oligomer region of the OH-stretching mode of ethanol dissolved in carbon tetrachloride is demonstrated, using two-color IR spectroscopy with excitation and probing pulses of 2 and 1 ps, respectively. The observed inhomogeneous broadening of the oligomer band is explained via local disorder of the hydrogen bonds. The lifetime of the spectral holes is estimated to be approximately 1 ps, providing evidence for rapid spectral relaxation and/or migration of vibrational excitation. The observed time evolution of excited state absorption from $v = 1$ to $v = 2$ levels yields the $v = 1$ population lifetime of 1.4 ± 0.3 ps. Breaking of the ethanol rings or chains as indicated by longer-lived induced absorption in the dimer/trimer region around 3450 cm^{-1} and further spectral features are reported.

Introduction

Intense, ultrashort pulses in the infrared spectral region allow time-resolved studies of vibrational dynamics in the condensed phase.[1] Improved versions of such techniques with two independently tunable IR pulses[2] and with polarization resolution[3] provide detailed spectroscopic insight. An important topic to be studied is hydrogen-bonded liquids, since little is known about the structural dynamics and vibrational relaxation of these systems. Because of its strong coupling and the large anharmonic frequency shift, the OH-stretching vibration can be used as a direct spectroscopic probe of H-bridge bonds.[4]

In this paper ethanol dissolved in CCl_4 is investigated using an advanced experimental system. The considerably better time resolution (factor of 6−8) as compared to earlier work reveals novel dynamical features, e.g., transient spectral holes followed by spectral relaxation in the oligomer band, the fast time evolution of excited state absorption, and the reorientational motion of excited oligomeric OH groups. Further advantages of the present investigation are the lower excitation level, avoiding possible perturbations by two-step (or even higher order) absorption processes of the intense pump radiation, and smaller thermalization effects that are readily distinguished from the primary molecular dynamics. Our investigation confirms several important features of the previous work, e.g. the rapid breaking of the hydrogen bonds after excitation of the stretching vibration of internal OH groups at 3330 cm^{-1}.[5] The present experimental system represents a compromise between time and frequency resolution requirements, and appears well suited to tackle the ultrafast dynamics and structural relaxation of hydrogen-bonded liquid systems.

Experimental Results

Our experimental system is only briefly described here and will be discussed in detail elsewhere.[6] We start with a pulsed, additive-pulse mode-locked Nd:YLF laser for the synchronous pumping of two optical parametric oscillators[7] in parallel. Single-pulse selection, frequency down-conversion, and amplification of the OPO outputs are carried out in subsequent optical parametric amplifier stages. In this way, tunable infrared excitation pulses of ≈2 ps duration and energy up to 10 μJ are generated in the range 2800−3700 cm^{-1}. Simultaneously, independently tunable probing pulses (duration 1 ps, energy < 1 μJ) are produced in a broad spectral band of 1600−3700 cm^{-1}. Two-color pump−probe absorption spectroscopy is carried out in the OH-stretching region with simultaneous detection of parallel (∥) and perpendicular (⊥) polarization components of the probe pulse with respect to the pump polarization. The pulses are close to the Fourier limitation as indicated by spectral widths of 8 cm^{-1} (pump) and 16 cm^{-1} (probe), respectively.

The sample solutions are prepared from commercially available ethanol (purity "pro analysi") and carbon tetrachloride (spectral grade "HPLC") without further purification. An ethanol concentration of 7 vol % (1.2 M) is chosen for a sample thickness of 100 μm corresponding to a minimum sample transmission of 0.12 at 3330 cm^{-1}. All measurements are performed at room temperature. Conventional IR absorption data are taken with a commercial Fourier transform spectrometer. The well-known absorption spectrum in the OH-stretching region is depicted in Figure 1c (dash−dotted line). The broad oligomer band centered at 3335 cm^{-1} represents OH groups in internal positions in oligomer rings and/or chains, while OH end groups with proton donor function and/or dimers are positioned around 3500 cm^{-1}. The small absorption at the frequency position 3630 cm^{-1} of monomers and OH end groups with proton acceptor function is not shown. Ethanol trimers, tetramers/pentamers, and larger polymers are characterized by spectral positions of the stretching vibration of internal OH groups of approximately 3450, 3330, and 3240 cm^{-1}, respectively.[8]

The time-resolved experiments are conducted with moderate pump energies of several microjoules and a frequency setting within the full width of the oligomer band, producing small depletions of the vibrational ground state of a few percent, only. Probing energies are reduced to a few nanojoules, 3 orders of magnitude below the excitation level. The energy transmission $T(\nu)$ of the probing pulse at frequency position ν through the excited sample is measured for parallel and perpendicular polarization and compared with the sample transmission $T_0(\nu)$

[⊗] Abstract published in *Advance ACS Abstracts,* April 15, 1997.

S1089-5639(96)01718-5 CCC: $14.00

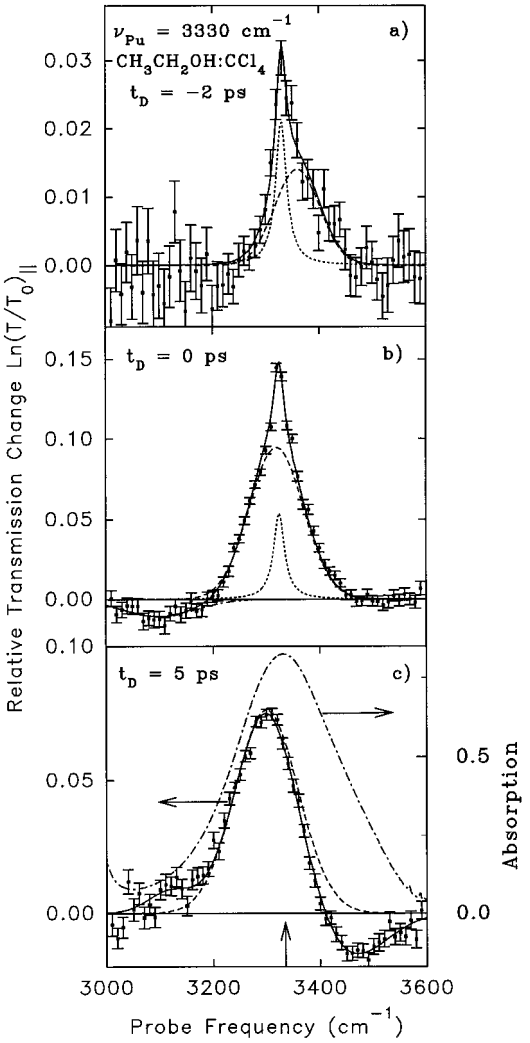

Figure 1. Transient probe spectra of ethanol dissolved in CCl_4 for parallel polarization of the excitation and probing pulses at three different delay times: −2 (a), 0 (b), and +5 ps (c); excitation at 3330 cm^{-1} (see vertical arrow). The relative transmission change of the probing pulse is plotted as a function of frequency position (experimental points); note the different ordinate scales. The curves are computed from a numerical model: Gaussian shaped oligomer bleaching (dashed); transient hole with Lorenztian shape (dotted); total spectrum (solid line). The conventional IR absorption band is shown for comparison (dash−dotted curve, right-hand side ordinate scale with absorbance units).

for blocked excitation beam. The resulting relative transmission changes $\ln(T/T_0)_{||,\perp}$ for variable probe frequency ν and probe delay time t_D are used in the following as the relevant signal quantities representing a direct measure of the molecular dynamics. From the two different polarization contributions of the probe pulse we are able to deduce an isotropic signal, $(\ln(T/T_0)_{||} + 2\ln(T/T_0)_{\perp})/3$, and the induced anisotropy signal, $(\ln(T/T_0)_{||} - \ln(T/T_0)_{\perp})/(\ln(T/T_0)_{||} + 2\ln(T/T_0)_{\perp})$. The temporal evolution of the induced anisotropy is governed by the time constant τ_{anis} while the isotropic signal delivers information on the molecular number densities and population dynamics.

In Figure 1 three transient spectra are depicted for excitation of internal OH groups in the oligomer band by pump pulses at 3330 cm^{-1} and probing at different, constant delay times. The relative transmission change is plotted versus probe frequency ν. At an early time of $t_D = -2$ ps (Figure 1a) evidence for transient spectral hole burning is obtained. A narrow spike is clearly indicated by the experimental points with approximately Lorentzian shape riding on a broader, Gaussian shaped structure. The decomposition into two constituents as suggested by a numerical analysis is shown in the figure (dotted and dashed lines). A hole width of 22 ± 4 cm^{-1} is inferred from the data after deconvolution of the instrumental resolution; the latter is governed by the bandwidth of the IR pulses. The bleaching seen even at this early delay time before the maximum of the excitation pulse originates from a decrease in the population difference between the $v = 0$ and $v = 1$ states of internal OH groups of oligomers containing four or more ethanol molecules. At $t_D = 0$ (Figure 1b) the bleaching in the oligomer region has grown to nearly 15% while hole burning is still visible. The two spectral components (dotted and dashed curves) fitting the experimental data (computed solid line) are displayed in the figure. In the red part of the transient spectrum below 3200 cm^{-1} an induced absorption is found as indicated by the negative transmission change.

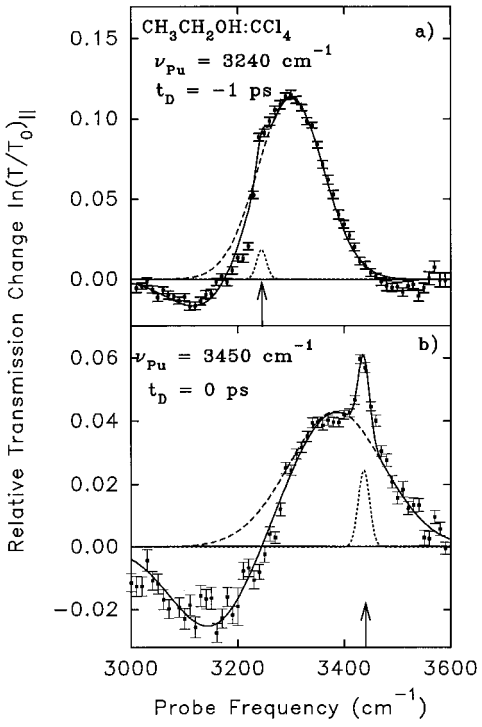

Figure 2. Same as Figure 1 for excitation at 3240 cm^{-1} and delay time −1 ps (a), and 3450 cm^{-1} and zero delay time (b).

Increasing the delay time to +5 ps (Figure 1c), the spectral hole has disappeared while the broader bleaching band still exists; it survives for relatively long times >80 ps (data not shown). The induced absorption in the red wing of the transient spectrum has been converted to a bleaching, peaked at 3180 cm^{-1}. In the blue part, on the other hand, an induced absorption centered at 3450 cm^{-1} has built up.

Transient spectra taken with excitation in the wings of the oligomer band at $\nu_{Pu} = 3240$ cm^{-1} and $\nu_{Pu} = 3450$ cm^{-1} are depicted in Figure 2. The spectra refer to early delay times of $t_D = -1$ ps and $t_D = 0$ ps, respectively. A shift of the transient hole with pump frequency is readily seen, while the hole-burning amplitude decreases in the red wing of the band, in spite of the expected increase of the transition dipole moment for larger red shifts of the OH vibration. The hole width is again measured to be 22 ± 4 cm^{-1} after deconvolution of the instrumental broadening. The peak position of the broad bleaching component (dashed curves) at these early delay times follows to some extent the excitation frequency, as seen in the figure. In contrast to the bleaching structures the induced absorption centered at 3100 cm^{-1} is not affected in position and line width by the variation of the pump frequency.

Some results on the time evolution of the absorption changes

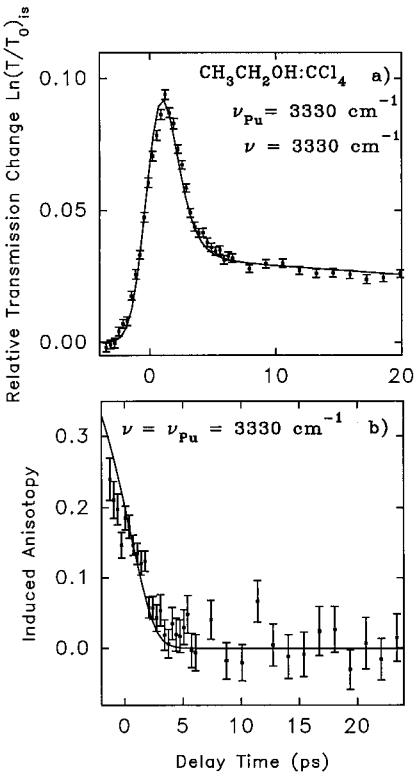

Figure 3. Relative transmission change of the probing pulse versus delay time for excitation at 3330 cm^{-1} and different polarization conditions: isotropic signal component (a) and normalized anisotropic component (b); experimental points, calculated curves; see text.

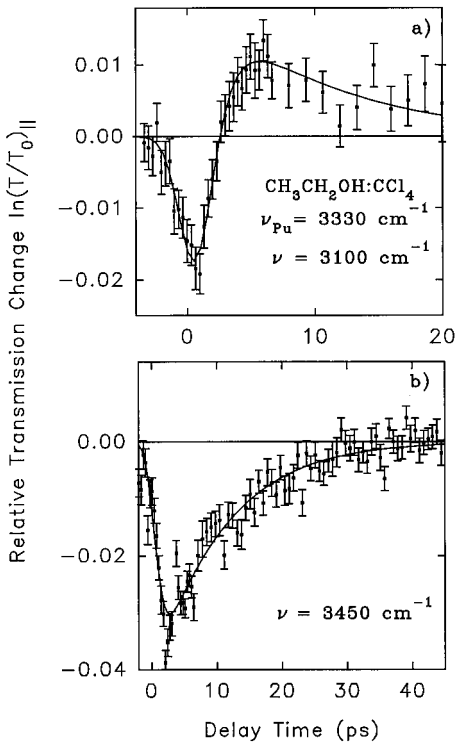

Figure 4. Same as Figure 3 for parallel polarization of pump and probing pulses and excitation at 3330 cm^{-1}. (a) Probing at 3100 cm^{-1} observing excited state absorption followed by a bleaching in the red wing of the oligomer band; (b) probing in the blue wing at 3455 cm^{-1}; the induced absorption indicates the breaking of ethanol oligomers; experimental points, computed curves; see text.

are presented in Figure 3, taken in the center of the oligomer band with $\nu = \nu_{Pu} = 3330$ cm^{-1}. The isotropic part of the signal component is depicted in Figure 3a. A rapid rise of the induced bleaching is noticed within experimental time resolution to a slightly delayed maximum at $t_D \approx 1$ ps. A first, fast decay with $\tau_h = 1.0 \pm 0.3$ ps follows, and a subsequent slow decline with a time constant of 80 ± 15 ps; the latter represents the lifetime of the broad bleaching component (dashed curves in Figure 1) while the former time constant obviously has to be connected with the spectral hole. The induced anisotropy shown in Figure 3b is derived from the same experimental data as for Figure 3a; it vanishes rapidly with a time constant $\tau_{anis} = 2.0 \pm 0.4$ ps. It should be noted that the zero delay time setting between pump and probe pulses has been determined in independent measurements.

Figure 4 illustrates in more detail the time evolution of the sample transmission for two prominent frequency settings of the probe pulse, while excitation is still performed at 3330 cm^{-1}. The signal transient depicted in Figure 4a is taken at $\nu = 3100$ cm^{-1} in the red wing of the oligomer band; the excited state transition ($\upsilon = 1$ to $\upsilon = 2$) is also expected in this frequency range. The measured transmission changes now exhibit a more complicated behavior. Around zero delay the induced absorption builds up rapidly within experimental time resolution that was already mentioned in context with Figure 1b. The signal minimum is slightly delayed relative to $t_D = 0$. The feature subsequently disappears quickly and changes into a bleaching amplitude related to the shoulder in the red part of the broad band in Figure 1c. The increased probe transmission vanishes in turn within 15 ± 10 ps.

Finally the induced absorption is investigated, probed at 3450 cm^{-1} in the blue wing of the oligomer band (see Figure 4b). This absorption feature builds up with a certain time delay compared to the induced absorption of Figure 4a (note different abscissa scales), indicating a secondary process. The observation is taken as evidence for the production of additional OH groups (in the vibrational ground state) at this frequency position. The phenomenon subsequently disappears again with a time constant of $\tau_{as} = 10 \pm 2$ ps.

Discussion

In order to deduce quantitative information from the measured probe spectra and signal transients, we propose a five-level model which is depicted schematically in Figure 5. The short, intense excitation pulse at 3330 cm^{-1} interacts with a subensemble of oligomeric OH groups in internal positions in the vibrational ground state (0) producing transitions to the first excited vibrational level (1) seen in the spectrum as a transient spectral hole. The pumping process is indicated by a thick vertical arrow in the figure. The excited subensemble relaxes in the following via spectral redistribution and/or energy transfer into a broader oligomer ensemble maintaining the population of the excited vibrational state (2). As the vibrational energy exceeds the hydrogen bond energy notably, and because of the distinct anharmonic coupling between the OH-stretching vibration and the bridge bond, dissociation of hydrogen bonds represents an important decay channel for the vibrational excitation. Via breaking of H bonds, smaller oligomers are formed with a corresponding number increase of OH end groups with proton donor function ("dimers") and trimers (level 3). The subsequent reassociation of dimers or trimers involves local temperature changes and is described by relaxation to level 4 representing a nonequilibrium distribution of H bonds at an increased temperature level, followed by slow thermalization processes. Probing transitions are indicated in Figure 5 by thin arrows, involving also $\upsilon = 2$ states of the OH vibration of internal groups and the $\upsilon = 1$ level of the broken oligomers. The dashed arrows illustrate the relaxation pathways. The

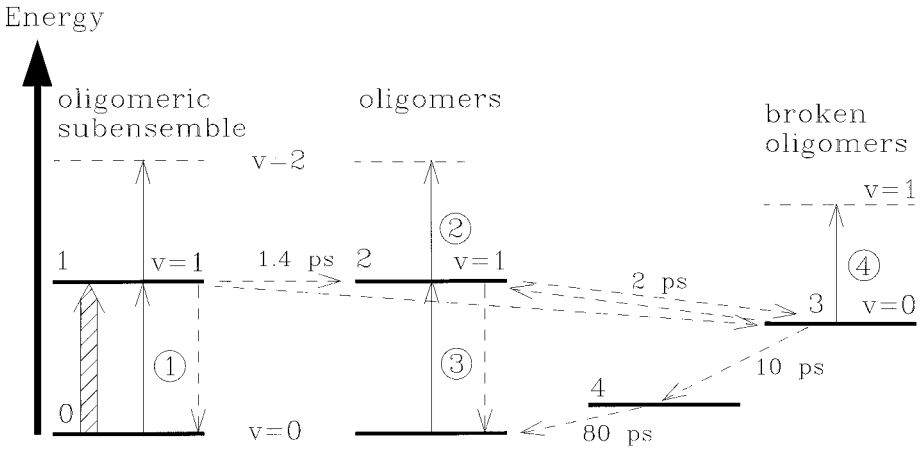

Figure 5. Energy level scheme of the theoretical model describing the dynamics of ethanol oligomers after IR excitation of the OH-stretching vibration (thick arrow) interacting with an oligomeric subensemble, only. The probing transitions (thin arrows) and relaxation pathways (dashed arrows) are indicated; for details see text.

reassociation of the broken oligomers with time constant τ_{as} is included in the model. Additional processes, i.e., further rearrangements of the hydrogen-bonded molecular system initiated by the pumping process and the thermalization of the deposited vibrational energy, are not considered in our simplified model.

The populations of levels 0−4 are treated by corresponding rate equations. For the transition between levels 0 and 1 the induced transition dipole moments are taken into account because of the relatively narrow spectral holes as compared to the spectral width of our IR pulses; i.e., the coherent response of the transition is included into the computations. The orientational distribution is incorporated into the calculations using the approximation of small population changes.[9] The transient spectra are computed assuming a Gaussian bandshape for the excited oligomer ensemble (transition between levels 2 and 3) while the shape of the spectral hole is taken to be Lorentzian. The curves in Figures 1−4 are calculated from the model; the Levenberg−Marquardt algorithm[10] is used for the fitting procedure. In the following we will discuss several features in more detail:

(i) The decay time of the induced anisotropy of the ethanol oligomers, $\tau_{anis} = 2.0 \pm 0.4$ ps (Figure 3b), is governed by reorientational motion, spectral relaxation, and/or transfer of vibrational quanta to other OH groups. For ethanol monomers in CCl_4 environment (concentration 0.3% volume), where the last two factors are irrelevant, the molecular reorientation time was measured to be 2.0 ± 0.5 ps using time-resolved IR spectroscopy with 10 ps pulses.[11] From NMR a value of 18 ps was determined for the rotational correlation time of 1 M ethanol in CCl_4.[12] The latter time constant represents an average value of all ethanol molecules in various H-bonding situations, the majority forming oligomers. At low concentration, i.e., for the monomers, a time constant of 6 ps was deduced from the NMR measurements by these authors. Although the difference of the numbers for the monomers derived from the two methods is not fully understood at present, the numbers suggest a considerably longer reorientation time for the oligomeric groups than for the monomers, as physically plausible. It is concluded that our value of τ_{anis} essentially represents spectral relaxation and/or energy transfer, with a minor contribution by the reorientational motion, only.

(ii) The induced absorption at 3100 cm^{-1} (Figure 1b) is attributed to excited state absorption (ESA) from $v = 1$ to $v = 2$ levels of the OH-stretching mode and taken as a direct measure of the excited state population, generated by the pump pulse. The time constant deduced from the corresponding signal transient (Figure 4a) is consequently interpreted as the population lifetime that is determined to be $T_1 = 1.4 \pm 0.3$ ps from the corresponding isotropic data. The ESA method employed here for T_1 is considered to be more reliable than the analysis of the bleaching signal of the oligomer band (fundamental transition), as used in the earlier investigation.[5] The larger value of T_1 estimated previously may be explained by superimposed processes due to the significantly enhanced excitation level, the much more pronounced thermalization effects for pumping with 10 ps pulses, and/or experimental time resolution problems. The following processes may contribute to the fast population decay rate $1/T_1$: breaking of hydrogen bonds (see below), energy transfer to other vibrational levels of ethanol, e.g., CH-stretching modes,[13] and transfer to solvent molecules. The large bandwidth of 160 cm^{-1} of the ESA and its independence of the pump frequency (see Figure 2) strongly suggest that the measurement of T_1 is not effected by spectral relaxation phenomena.

The ESA band is red-shifted by $\Delta\nu = 230 \pm 20$ cm^{-1} compared to the oligomer band. This large shift is consistent with the enhanced anharmonic character of the stretching mode of internal OH groups as compared to the measured shift for ethanol monomers of 170 cm^{-1}.[11,14] The slower dynamics of the bleaching amplitude at later times in Figure 4a obviously does not represent ESA but a different dynamical feature in the red wing of the oligomer band, also indicated by the shifted position of the maximum transient bleaching compared to the conventional spectrum in Figure 1c (see below). The latter dynamics may be related to a rearrangement of the hydrogen-bonded distribution, once the chemical equilibrium has been perturbed by the deposition of vibrational energy.

(iii) The observed transient spectral holes in the oligomer band present direct evidence for the inhomogeneous broadening generated by hydrogen bonds and are demonstrated here for a liquid at room temperature for the first time. The hole width of 22 ± 4 cm^{-1} (fwhm) is found to be constant within experimental accuracy during the observation time of a few picoseconds. This value is considerably smaller than found previously for the OH dimer band of a polymer at room temperature;[15] the difference by a factor of approximately 4 may be accounted for by more pronounced motional narrowing in the liquid and also by a larger frequency value of the bridge-bond stretching vibration.

In order to rule out a possible coherence peak contribution to the transient signal for equal pump and probe frequency, several measurements were carried out with varying pump amplitude. Reducing the pump intensity by a factor of 4, we found no measurable difference in the ratio between the peak

amplitude and the long-lived signal value. The maximum hole-burning amplitude is observed notably delayed to $t_D = 0$. A coherent coupling artifact via the nonresonant part of the third order nonlinear susceptibility is clearly excluded by measurements of the neat solvent. These findings indicate that a coherence peak is negligible in our measurements.

(iv) The measured lifetime of the transient holes of $\tau_h = 1.0 \pm 0.3$ ps is shorter than the population lifetime. Two effects may account for the difference: spectral relaxation via structural changes around the individual excited OH groups and/or vibrational energy transfer to neighboring ethanol molecules maintaining the population of the OH mode, i.e., migration of the vibrational quanta to hydroxylic groups with different spectral positions. It should be noted that the latter mechanism is restricted to excess population of OH groups in the $v = 1$ level; spectral relaxation, on the other hand, may occur also for population holes in the vibrational ground state (generated, e.g., by breaking of H bonds). The presence of an additional fast process besides population decay is strongly supported by the observation of a rapidly decaying anisotropy (Figure 3b) and of a second, broad bleaching component in the oligomer band, slightly blue-shifted from the excitation frequency (see Figure 1a,b). Some more details will be discussed below.

(v) A further striking feature of the transient spectra is the induced absorption around 3450 cm^{-1}, rising rapidly but slightly delayed with respect to the ESA signal (Figures 1c and 4b). The signal amplitude directly indicates excess molecules in the vibrational ground state at this frequency position that can occur only via breaking of H bonds, i.e., vibrational predissociation. The spectral region is assigned to dimers, trimers, and/or OH end groups with proton donor function.[16] From the transient spectra we estimate a bandwidth of the absorption peak of 160 $\pm$ 20 cm^{-1} as compared, for example, to the reported width of the trimer absorption of 40 cm^{-1}.[16] The different species that may be produced by the breaking of cyclic oligomers and/or long ethanol chains are not distinguished because of the large spectral congestion. The blue-shift of the peak value from the spectral position of end groups with donor function (3500 cm^{-1}) suggests a distinct trimer contribution. Computations of the transient spectra in the time interval $-2 \leq t_D \leq 10$ ps for excitation at 3330 cm^{-1} with the model of Figure 5 and comparison with experimental data yield for the breaking of the ethanol tetramers/pentamers a time constant of $\tau_{dis} = 2.0 \pm 0.2$ ps while the reverse process is negligible, as suggested by detailed balance arguments.

The predissociation time constant of 2 ps can be compared with theoretical expectations. Staib and Hynes recently studied the dissociation of H-bonded dimers in the $v = 1$ level of the OH-stretching mode.[17] These authors consider an adiabatic model for the vibrational predissociation based on semiempirical potential functions. The time constant of dissociation for ethanol dimers is estimated to be $\approx$12 ps, strongly dependent on the strength of the H bond. A faster predissociation is predicted for a stronger bond or correspondingly larger red-shift of the OH vibration relative to the monomer frequency, $\tau_{dis} \propto \delta\nu^{-1.8}$. Using these results for the dissociation of internal OH groups ($\delta\nu \approx 300$ cm^{-1}), one estimates $\tau_{dis} \approx 2.5$ ps in satisfactory agreement with the experimental value.

Subsequent reassociation of the dimers/trimers to the vibrational ground state of the ethanol tetramers/pentamers obviously occurs within $\tau_{as} = 10 \pm 2$ ps. Compared to earlier findings with longer pulses of 10 ps,[5] the reassociation is faster by a factor of $\approx$2 and more complete, i.e., displays a smaller asymptotic amplitude consistent with the lower energy deposition and notably weaker thermalization effect under the present experimental conditions.

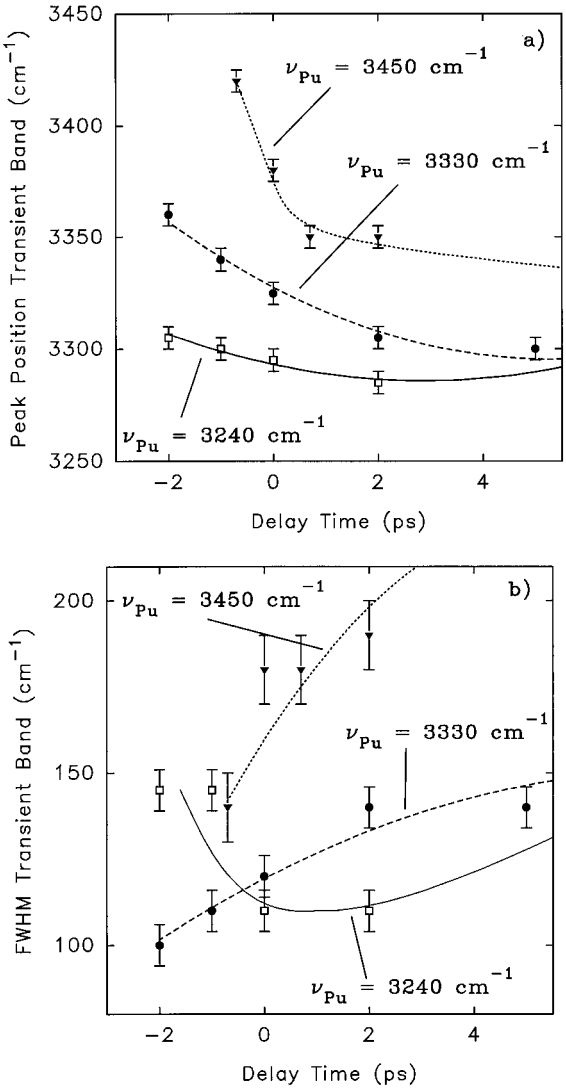

Figure 6. Time evolution of the broad bleaching component in the oligomer band of ethanol; peak position (a) and bandwidth (b) as derived from the numerical analysis of the transient spectra plotted versus delay time for three excitation frequencies: 3240 cm^{-1} (open squares), 3330 cm^{-1} (filled circles), and 3450 cm^{-1} (filled triangles); experimental points; lines are drawn as a guide to the eye.

We now turn to the discussion of further experimental findings. The broad bleaching component in the oligomer band (see Figures 1 and 2) is of particular interest. That part of the spectral feature connected to $v = 1$ population also provides a possible explanation for the broad ESA band discussed above, since an initial narrower spectral feature ("inverse hole") of the ESA may be washed out by the limited experimental time resolution. Some data on the time evolution of the broad bleaching component are presented in Figure 6 (data for larger delay times not shown). The peak position (Figure 6a) and bandwidth (Figure 6b) as derived from the numerical analysis of the transient spectra are plotted versus delay time for three different pump frequencies within the oligomer absorption band. With increasing excitation frequency the temporal evolution of the bleaching component is more pronounced: pumping in the blue wing, where the dimers/trimers and/or OH end groups with proton donor function are positioned, we find a first fast red-shift of the bleaching component of 80 cm^{-1} while the bandwidth simultaneously increases up to 190 cm^{-1}. The fast changes are followed by a slower approach to the equilibrium

values of the oligomer band. Excitation of ethanol chains or rings at $\nu_{Pu} = 3330$ cm^{-1} results in a somewhat slower dynamical behavior: the transient bleaching displays a frequency downshift and bandwidth increase within several picoseconds while the subsequent time evolution toward the equilibrium numbers occurs on a longer time scale of the order of 100 ps (not shown in Figure 6). For pumping in the red wing of the oligomer band with $\nu_{Pu} = 3240$ cm^{-1}, the peak of the oligomer bleaching at 3300 cm^{-1} is only weakly time-dependent around zero delay time, while the bandwidth decreases within 4 ps from 150 to 115 cm^{-1}.

A possible explanation may be given along the following lines: apart from the early hole-burning dynamics, excitation and breaking of mainly ethanol tetramers/pentamers at $\nu_{Pu} = 3330$ cm^{-1} result in the generation of dimers and trimers. The latter species have two possibilities to react: (1) reassociation of the fragments to ethanol tetramers/pentamers as observed experimentally with a time constant of $\tau_{as} = 10$ ps; (2) association with tetramers/pentamers to form even longer ethanol chains or rings, characterized by corresponding red-shifted spectral positions. The process may explain the delayed induced bleaching around 3180 cm^{-1} (Figure 4a) and play also a role for the time-dependent red-shift of the broad transient bleaching and its increasing bandwidth (Figure 6). The present authors believe that the dynamics after the first 5 ps becomes rather complex. A detailed interpretation and an analysis of the thermalization processes is not attempted on the basis of the available data.

Conclusions

We have observed transient spectral holes in the oligomer band of ethanol dissolved in CCl_4 demonstrating the inhomogeneous character of the OH-stretching vibration due to structural disorder via hydrogen bonds. From time-resolved measurements of the excited state absorption, the lifetime $T_1 = 1.4 \pm 0.3$ ps is directly determined for the $v = 1$ level of internal OH groups of oligomers. The dominant decay channel is the breaking of hydrogen bonds generating excess absorption in the dimer/trimer region. The predissociation time is estimated to be $\approx$2 ps, followed by reassociation with 10 ± 2 ps. The spectral holes are accompanied by a broader bleaching component in the oligomer band that provides evidence for rapid spectral relaxation and/or vibrational energy redistribution of hydroxylic groups. The latter processes are also indicated by the short time constant of the induced optical anisotropy, $\tau_{anis} \approx 2$ ps, since NMR and other data suggest the molecular reorientation is notably slower.

References and Notes

(1) Spanner, K.; Laubereau, A.; Kaiser, W. *Chem. Phys. Lett.* **1976**, *44*, 88. Heilweil, E. J.; Casassa, M. P.; Cavangh, R. R.; Stephenson, J. C. *J. Chem. Phys.* **1986**, *85*, 5004. Li, M.; Owrutsky, J.; Sarisky, M.; Culver, J. P.; Yodh, A.; Hochstrasser, R. M. *J. Chem. Phys.* **1993**, *98*, 5499. Tokmakoff,A.; Zimdars, D.; Urdahl, R. S.; Francis, R. S.; Kwok, A. S.; Fayer, M. D. *J. Phys. Chem.* **1995**, *99*, 13310.

(2) Graener, H.; Dohlus, R.; Laubereau, A. *Chem. Phys. Lett.* **1987**, *140*, 306.

(3) Graener, H.; Seifert, G.; Laubereau, A. *Chem. Phys. Lett.* **1990**, *172*, 435.

(4) Graener, H.; Seifert, G.; Laubereau, A. *Phys. Rev. Lett.* **1991**, *66*, 2092. Bonn, M.; Brugmans, M. J. P.; Kleyn, A. W.; van Santen, R. A.; Bakker, H. J. *J. Chem. Phys.* **1996**, *105*, 3431. Bonn, M.; Bakker, H. J.; Kleyn, A. W.; van Santen, R. A. *J. Phys. Chem.* **1996**, *100*, 15301. Arrivo, S. M.; Heilweil, E. J. *J. Phys. Chem.* **1996**, *100*, 11975.

(5) Graener, H.; Ye, T. Q.; Laubereau, A. *J. Chem. Phys.* **1989**, *90*, 3413.

(6) Laenen, R.; Rauscher, C. Unpublished results.

(7) Rauscher, C.; Roth, T.; Laenen, R.; Laubereau, A. *Opt. Lett.* **1995**, *20*, 2003.

(8) Barnes, A. J.; Hallam, H. E. *Trans. Faraday Soc.* **1970**, *66*, 1932.

(9) Band, Y. B. *Phys. Rev.* **1986**, *A34*, 326.

(10) Press, W. H. *Numerical Recipes*; Cambridge University Press: Cambridge, 1986.

(11) Ye, T.-Q. Dissertation, Universität Bayreuth, Germany, 1991.

(12) Ludwig, R.; Zeidler, M. D. *Mol. Phys.* **1994**, *82*, 313.

(13) Graener, H.; Ye, T.-Q.; Laubereau, A. *J. Chem. Phys.* **1989**, *91*, 1043.

(14) Luck, W. A. P.; Ditter, W. *Ber. Bunsen-Ges. Phys. Chem.* **1968**, *72*, 365.

(15) Graener, H.; Ye, T.-Q.; Laubereau, A. *Phys. Rev.* **1990**, *B41*, 2597.

(16) van Thiel, M.; Becker, E. D.; Pimentel, G. C. *J. Chem. Phys.* **1957**, *27*, 95.

(17) Staib, A.; Hynes, J. T. *Chem. Phys. Lett.* **1993**, *204*, 197.